

**Influence of Coprecipitated Organic Matter on $\text{Fe}^{2+}_{(\text{aq})}$ -Catalyzed Transformation
of Ferrihydrite: Implications for C Dynamics**

Chunmei Chen^{1*}, Ravi Kukkadapu², and Donald L Sparks¹

1. Department of Plant and Soil Sciences

Delaware Environmental Institute

University of Delaware, Newark, DE, USA 19711

2. Environmental Molecular Sciences Laboratory

Pacific Northwest National Laboratory, Richland, WA, USA 99354

Number of Pages: 20

Number of Figures: 10

Number of Tables: 4

Corresponding Author

*Phone: (302)8318345. Fax: (302)8310605. E-mail: cmchen@udel.edu

Materials and Methods

Composition of the initial DOM solution

The DOC concentration of the stock solution was determined by a TOC analyzer (Apollo 9000HS). The concentration of major cations in the initial DOM stock solution was analyzed by ICP-AES.

C K-edge NEXAFS analysis

The fluorescence yield data was collected using a two stage microchannel plate detector. The $1s \rightarrow \pi^*$ C=O transition at 288.6 eV (Kim et al., 2003) of citric acid was used for calibration at the C K-edge.

A minimum of thirty five scans were averaged and normalized to the incident flux using scans of an Au-coated Si wafer. Measurements of the incident flux at the C K-edge were scaled and offset prior to normalization to mitigate the effect of flux attenuation by C contamination on beam optics (Watts et al., 2006). Spectra were background corrected with a linear regression fit through the pre-edge region and normalized to an edge jump of unity using custom macros (Gillespie et al., 2014) in IGOR Pro and Athena (Ravel and Newville, 2005) Software packages. Features at the C K-edge were assigned according to the literature (Chen et al., 2014a, 2014b).

Results and Discussion

Variable temperature Mössbauer spectroscopy data of pure ferrihydrite (C/Fe = 0) and OM-ferrihydrite coprecipitates (C/Fe = 1.2, and C/Fe = 1.6), were obtained to gain insights into extent of inter-particle interactions and their average particle size/crystallinity. The room temperature (RT) Mössbauer spectral parameters of pure-ferrihydrite doublet were CS (center shift) = 0.37 mm/sec and QS (quadrupole splitting)

= 0.80 mm/sec (SI Figures S2a and S3a; Table S1). The CS of OM-ferrihydrite coprecipitates were as expected virtually identical to pure ferrihydrite, while on the other hand their QS increased to 0.85 mm/sec (SI Figures S2 and S3; Table S1), indicating a distortion of octahedral geometry around the Fe atom (Eusterhues et al, 2007). These modeled-derived parameters and increase in QS with OM incorporation are in agreement with the study by Eusterhues *et al* (2007). Virtually identical C/Fe = 1.2 and C/Fe = 1.6 spectra further implied that the extent of OM content, at least in this range, had little or no effect on Fe(III) coordination environments.

The RT paramagnetic doublets are completely transformed to sextets at 5 K (SI Figure S2b). The modeled magnetic hyperfine field (B_{hf}) of FH (average of 48.1 T; SI Figure S3b and Table S1) is characteristic of 2-line ferrihydrite (Kukkadapu et al., 2003; Murad and Cashion, 2004). The OM-ferrihydrite sextet's average B_{hf} , on the other hand, are relatively lower than FH (45.4 T and 40.1 T for C/Fe = 1.2 and C/Fe = 1.6, respectively; SI Figure S2b; Figures S3b, d, f; Table S1). Such a decrease in B_{hf} is in line with weaker inter-particle interactions and is due to coating of FH with OM. The change in B_{hf} may also be related to decrease in average particle-size/crystallinity with increasing OM content (Eusterhues et al, 2007).

Mössbauer spectra were also obtained between 77 K and 5 K to better understand inter-particle interactions (Figure 1). Sorbed OM (or *e.g.*, SiO_4^{4-} , PO_4^{3-}) on ferrihydrite will not only decrease surface unpaired spins responsible for magnetic interactions with neighboring particles but also weaken the inter-particle magnetic interactions due to OM in the matrix (Joshi et al., 2015; Morup, 1994; Zhao et al., 1996). In other words, probability of a paramagnetic doublet at a certain temperature is higher if inter-particle

attractions are weaker or absent due to sorbed OM. The existence of doublets at lower temperatures in OM-ferrihydrite than pure ferrihydrite is in agreement with weaker inter-particle interactions in OM-containing samples (Figure 1). For example, doublet transformation to sextet occurred at 77-65 K for pure ferrihydrite. The transitions from doublet to sextet, on the other hand, were in 35-25 K and 25-15 K for OM-ferrihydrite samples with C/Fe ratios of 1.2 and 1.6, respectively. The decrease in this transition temperature or blocking temperature (a temperature where sextet to doublet spectral ratio is $\sim 1:1$ (Murad and Cashion, 2004)) is also a function of average particle size, decreases with decreasing particle size, and is related to superparamagnetic relaxation rate (Murad and Cashion, 2004). Mössbauer data spectra shown in Figure 1 (between 77 K and 5 K) were not modeled because of modeling spectra with unique doublet to sextet spectral ratio is rather complex. Overall, variable temperature Mössbauer spectroscopy study indicated that with increasing OM content, inter-particle interactions become weaker and average particle size decreases.

References

- 1) Chen, C.; Dynes, J.J.; Wang, J.; Karunakaran, C.; Sparks, D.L. 2014a. Soft X-ray Spectromicroscopy Study of Mineral-Organic Matter Associations in Pasture Soil Clay Fractions. *Environ. Sci. Technol.* **2014a**, 48(12), 6678-6686.
- 2) Chen, C.; Dynes J.; Wang, J.; Sparks, D.L. Properties of Fe-organic matter associations via coprecipitation versus adsorption. *Environ. Sci. Technol.* **2014b**, 48 (23):13751-13759.
- 3) Eusterhues, K.; Wagner, F. E.; Häusler, W.; Hanzlik, M.; Knicker, H.; Totsche, K. U.; Kögel-Knabner, I.; Schwertmann, U. Characterization of ferrihydrite-soil organic matter coprecipitates by X-ray diffraction and Mössbauer spectroscopy. *Environ. Sci. Technol.* **2008**, 42, 7891-7897.
- 4) Gillespie, A. W.; Diochon, A.; Ma, B. L.; Morrison, M. J.; Kellman, L.; Walley, F. L.; Regier, T. Z.; Chevrier, D.; Dynes, J. J.; Gregorich, E. G. Nitrogen input quality changes the biochemical composition of soil organic matter stabilized in the fine fraction: a long-term study. *Biogeochemistry* **2014**, 117, 337-350
- 5) Joshi, S. R.; Kukkadapu, R. K.; Burdige, D.; Bowden, M.; Sparks, D. L.; Joshi, D. P. Organic matter remineralization predominates phosphorus cycling in the mid-Bay sediment in the Chesapeake Bay. *Environ. Sci. Technol.* **2015**, 49(10), 5887-5896.
- 6) Kim, J. S.; Ree, M.; Lee, S. W.; Oh, W.; Baek, S.; Lee, B.; Shin, T. J.; Kim, K. J.; Kim, B.; Lüning, J. NEXAFS spectroscopy study of the surface properties of zinc glutarate and its reactivity with carbon dioxide and propylene oxide. *J. Catal.* **2003**, 218, 386-395.
- 7) Kukkadapu, R. K.; Zachara, J. M.; Fredrickson, J. K.; Smith, S. C.; Dohnalkova, A. C.; Russell, C. Transformation of 2-line ferrihydrite to 6-line ferrihydrite under oxic and anoxic conditions. *Am. Mineral.* **2003**, 88, 1903-1914.
- 8) Morup, S. Superferromagnetic nanostructures. *Hyperfine Interact.* **1994**, 90, 171-185.
- 9) Murad, E.; Cashion, J.; Mossbauer spectroscopy of Environmental Materials and their Industrial Utilization. *Kluwer Academic Publishers*, **2004**.
- 10) Ravel, B.; Newville, M. ATHENA, ARTEMIS, HEPHAESTUS: data analysis for X-ray absorption spectroscopy using IFEFFIT. *J. Synchrotron Radiat.* **2005**, 12, 537-541.
- 11) Watt, B.; Thomsen, L.; Dastoor, P. C. Methods in carbon K-edge NEXAFS: experiment and analysis. *J. Electron Spectrosc. Relat. Phenom.* **2006**, 151, 105-120.
- 12) Zhao, J.; Huggins, F. E.; Feng, Z.; Huffman, G. P. Surface-induced superparamagnetic relaxation in nanoscale ferrihydrite particles. *Physical Review B* **1996**, 54(5), 3403-3407.

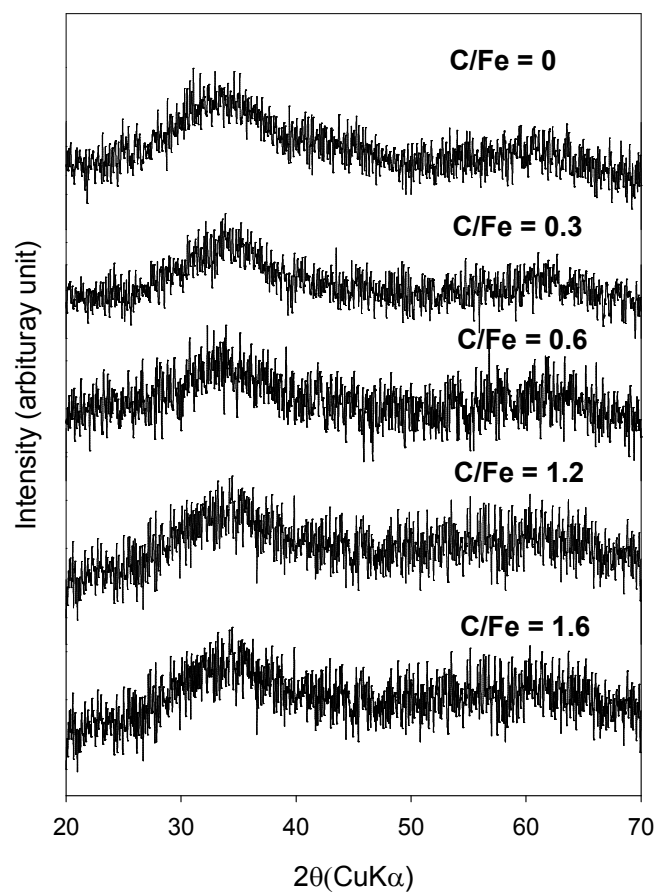


Fig.S1 XRD patterns of (OM-)ferrihydrite coprecipitates with C/Fe molar ratio of 0-1.6.

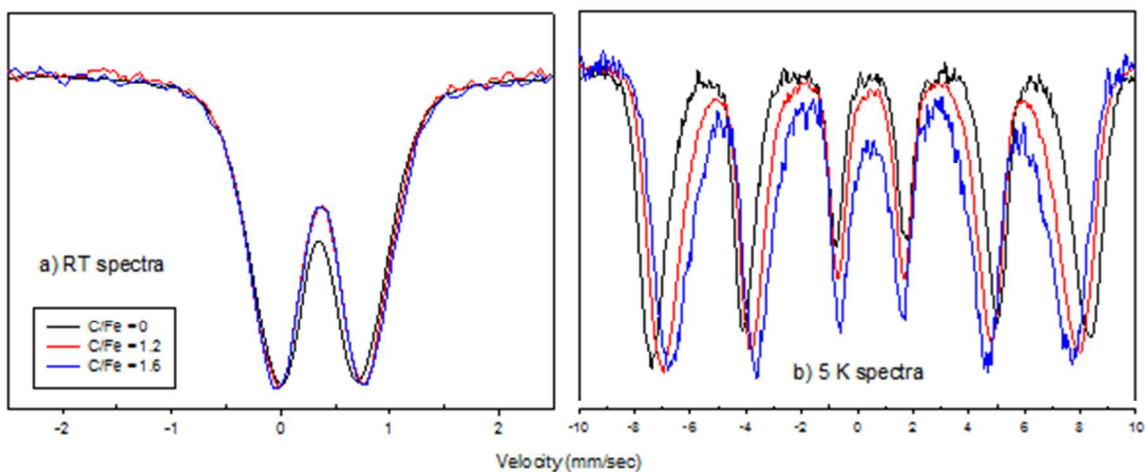


Fig.S2 Mössbauer spectra of pure ferrihydrite ($C/Fe=0$) and OM-ferrihydrite coprecipitates ($C/Fe=1.2$ and $C/Fe=1.6$): a) unmodeled room-temperature (RT) spectra illustrating differences between pure ferrihydrite ($C/Fe=0$) and OM-ferrihydrite coprecipitates ($C/Fe=1.2$ and $C/Fe=1.6$) and similarity between OM-ferrihydrite coprecipitates of $C/Fe=1.2$ and $C/Fe=1.6$, and b) unmodeled 5 K spectra showing difference in magnetic hyperfine field and peak widths.

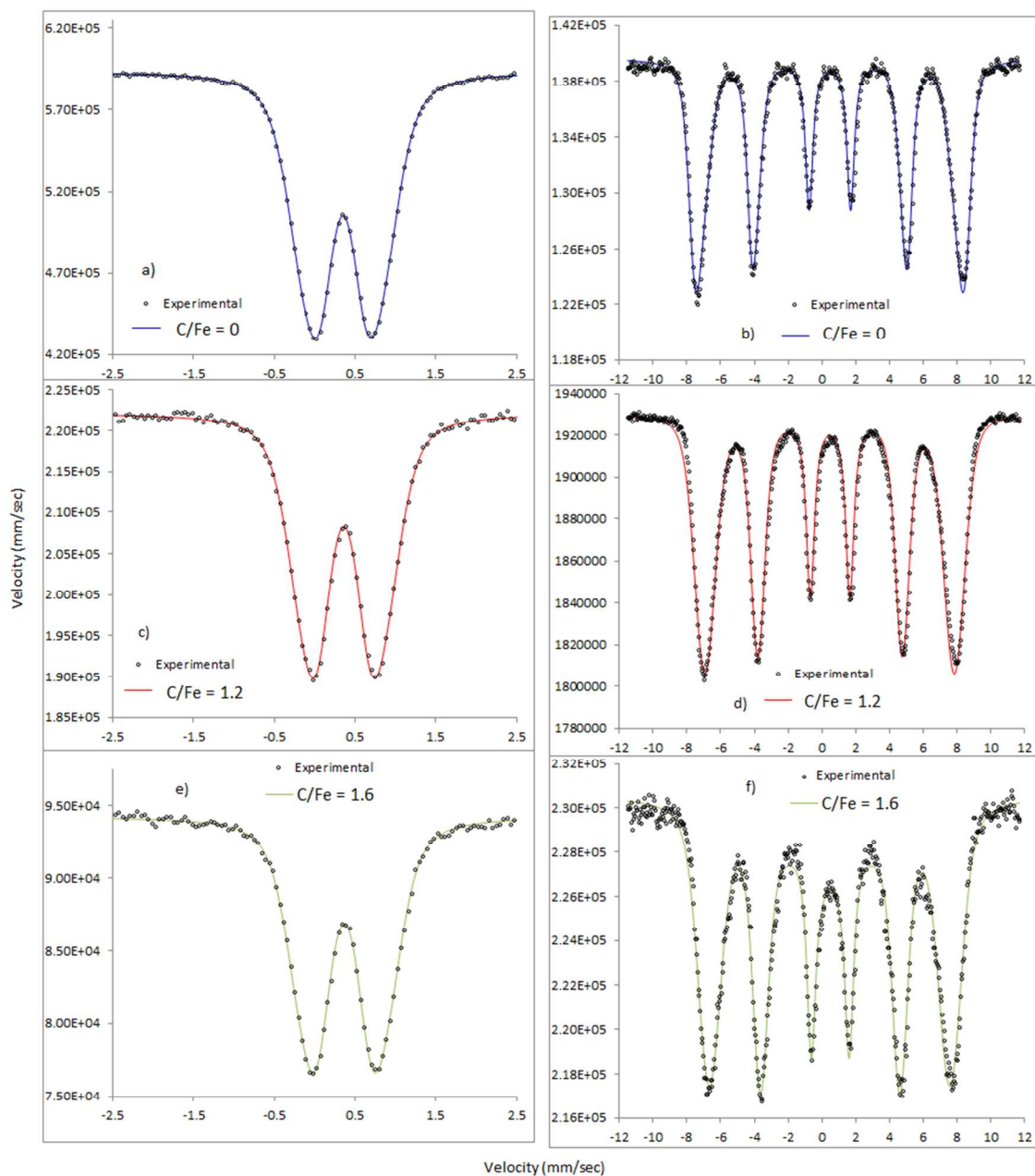


Fig.S3 Modeled Mössbauer spectra of pure ferrihydrite ($C/Fe=0$) and OM-ferrihydrite coprecipitates ($C/Fe=1.2$ and $C/Fe=1.6$) at (a, c & e) room temperature and (b, d & f) at 5 K, respectively.

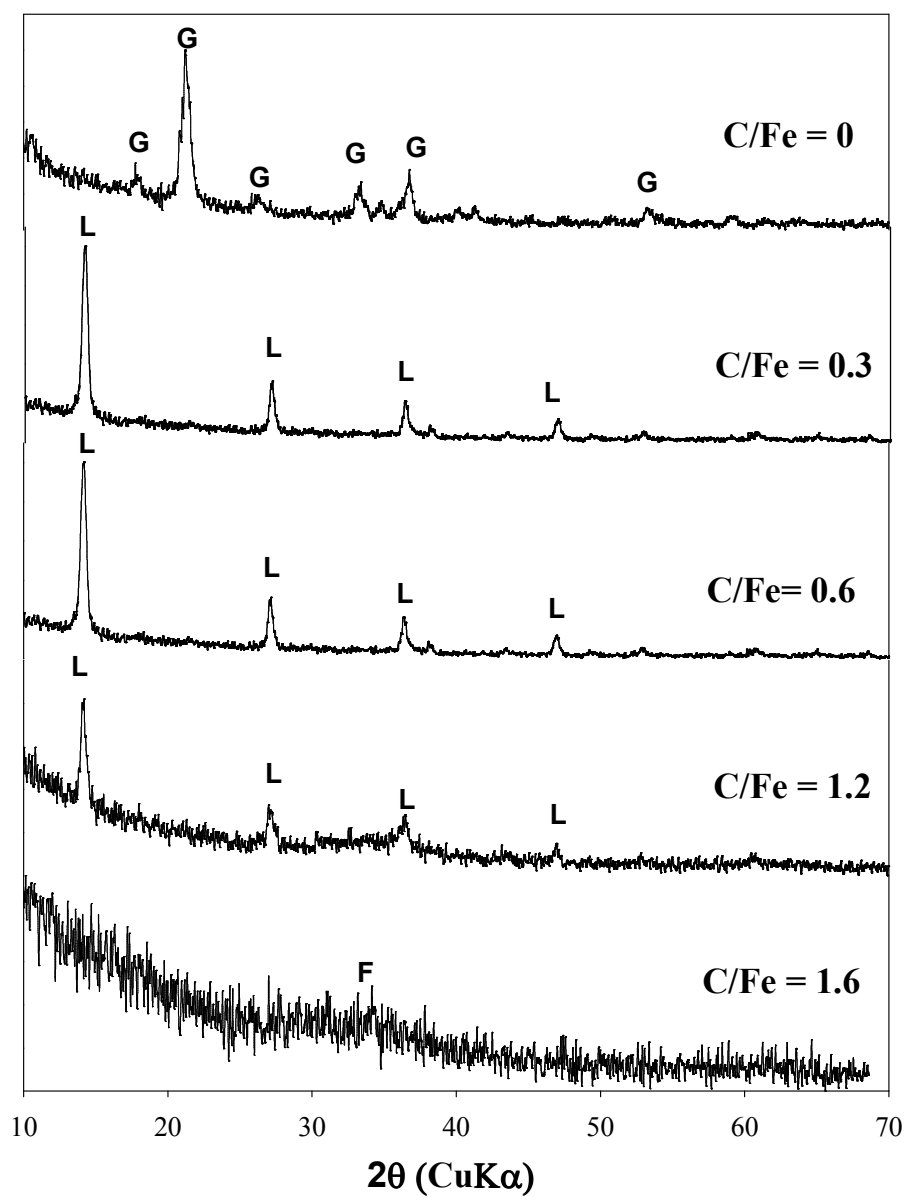


Fig.S4 XRD patterns of the secondary minerals formed following 90 days of reaction of 0.2 mM Fe(II) with (OM-)ferrihydrite coprecipitates containing C/Fe molar ratio of 0-1.6. F: Ferrihydrite; L, Lepidocrocite; G, Goethite.

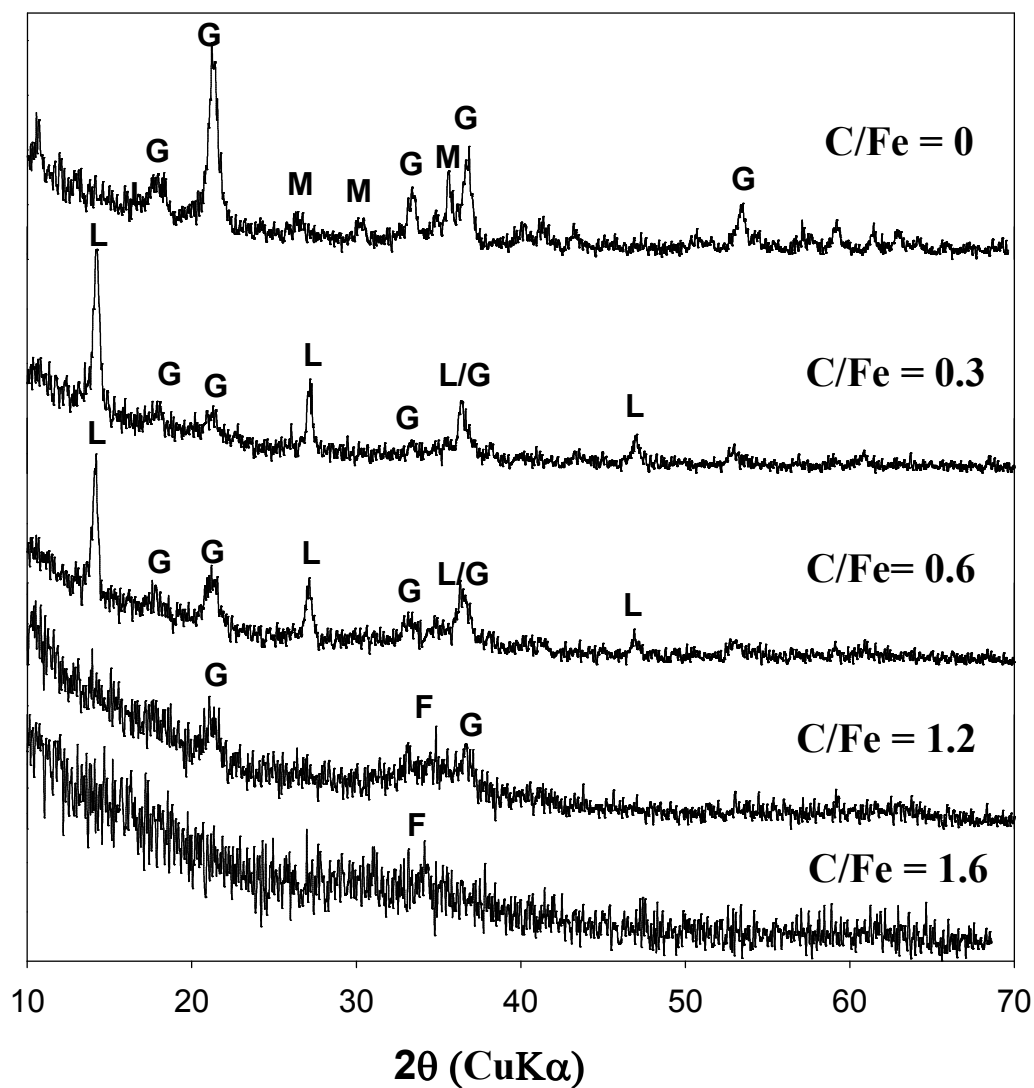


Fig.S5 XRD patterns of the secondary minerals formed following 90 days of reaction of 2 mM Fe(II) with (OM-)ferrihydrite coprecipitates containing C/Fe molar ratio of 0-1.6. F: Ferrihydrite; L, Lepidocrocite; G, Goethite; M, Magnetite.

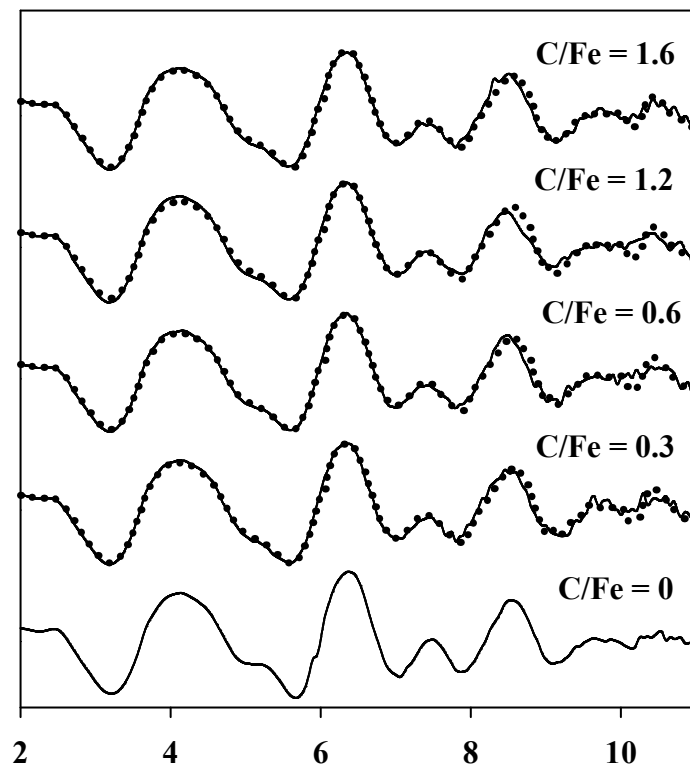


Fig.S6 Iron k^3 -weighted EXAFS spectra of pure ferrihydrite (C/Fe = 0) and OM-ferrihydrite coprecipitates containing C/Fe molar ratio of 0.3-1.6. Dotted lines show linear combination fits over k -range of 2-11 \AA^{-1} using pure ferrihydrite. The C/Fe molar ratio is indicated above the right area of the spectra.

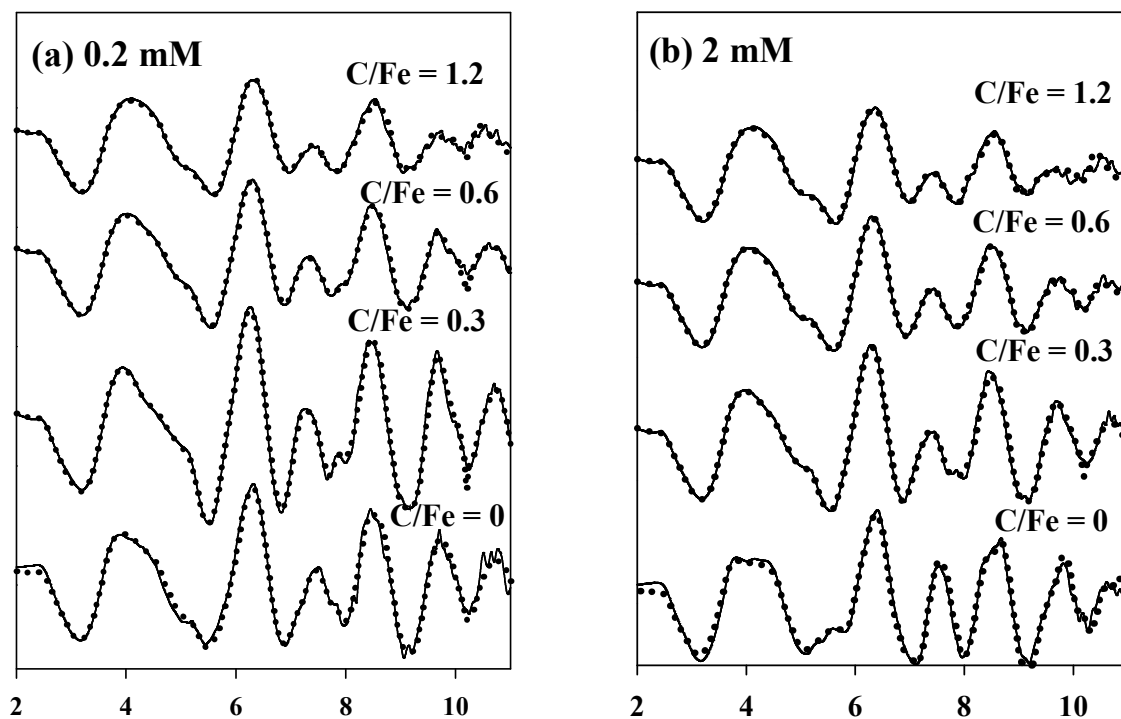


Fig.S7 Iron k^3 -weighted EXAFS spectra (solid line) and linear combination fits (dotted line) of the mineral percentage results (Fig.4 and Fig.5) for (OM-)ferrihydrite coprecipitates reacted with (a) 0.2 mM and (b) 2.0 mM aqueous Fe(II) for 18 hours. The C/Fe molar ratio of (OM-)ferrihydrite coprecipitates is indicated above the right area of the spectra.

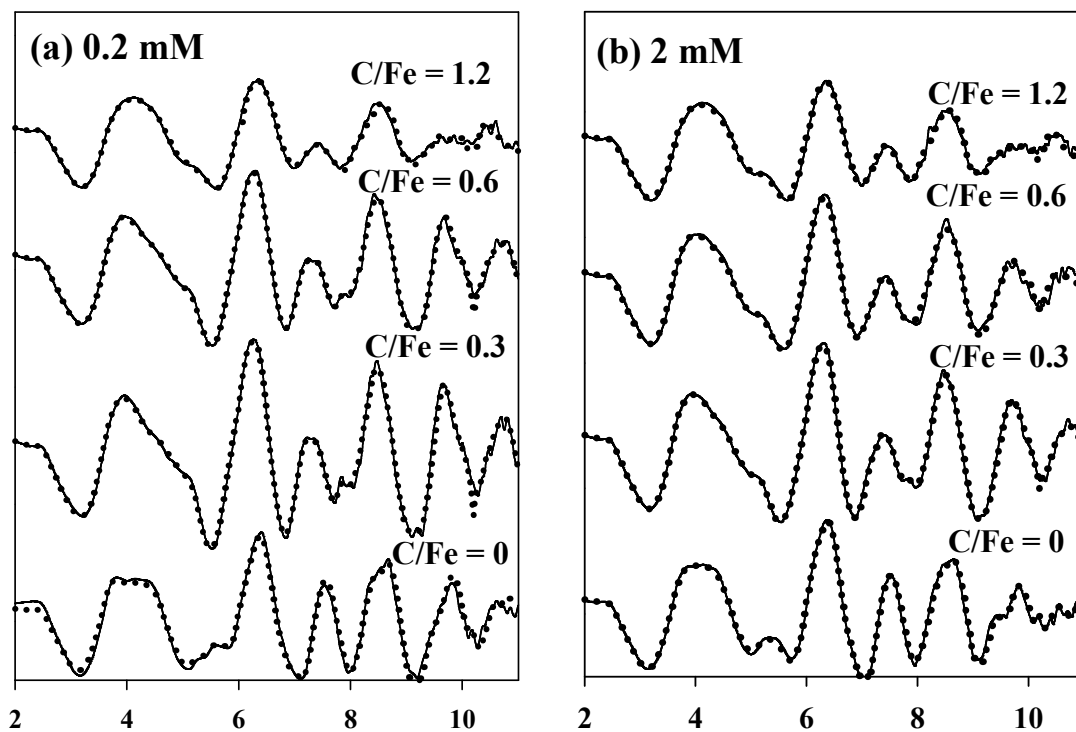


Fig.S8 Iron k^3 -weighted EXAFS spectra (solid line) and linear combination fits (dotted line) of the mineral percentage results (Fig.4 and Fig.5) for (OM-)ferrihydrite coprecipitates reacted with (a) 0.2 mM and (b) 2.0 mM aqueous Fe(II) for 6 and 10 days, respectively. The C/Fe molar ratio of (OM-)ferrihydrite coprecipitates is indicated above the right area of the spectra.

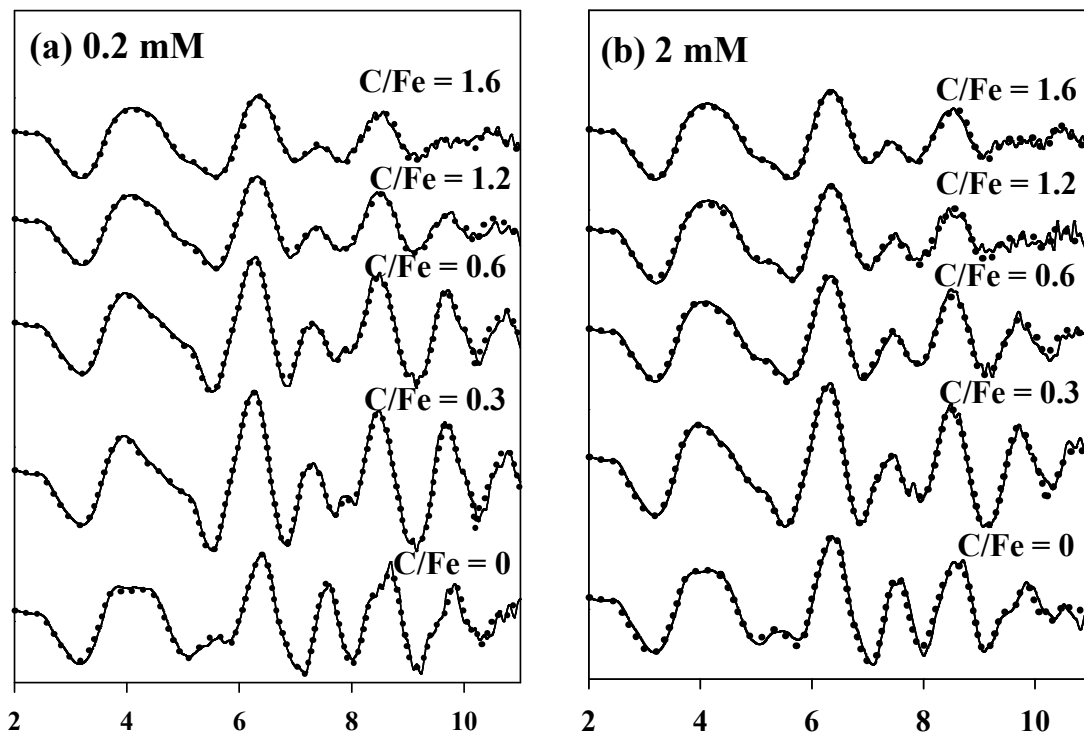


Fig.S9 Iron k^3 -weighted EXAFS spectra (solid line) and linear combination fits (dotted line) of the mineral percentage results (Fig. 2, Fig.4 and Fig.5) for (OM-)ferrihydrite coprecipitates reacted with (a) 0.2 mM and (b) 2.0 mM aqueous Fe(II) for 90 days, respectively. The C/Fe molar ratio of (OM-)ferrihydrite coprecipitates is indicated above the right area of the spectra.

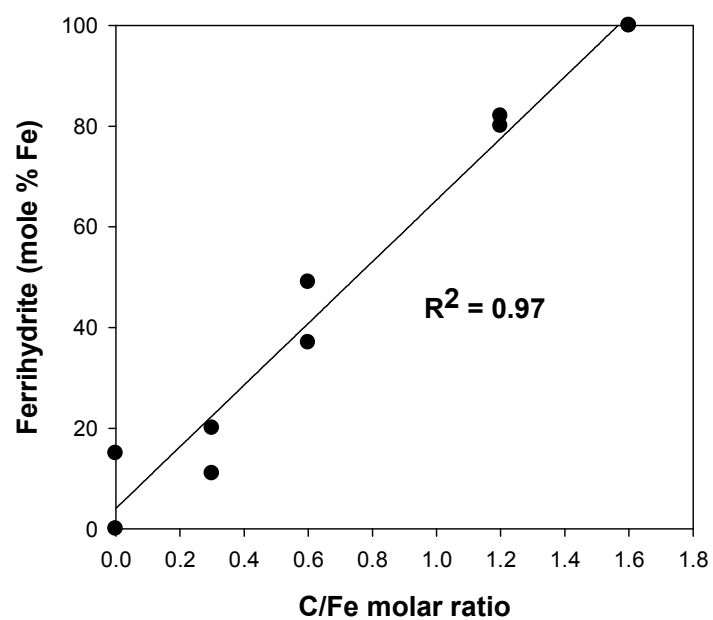


Fig.S10 Preservation of ferrihydrite as a function of C/Fe molar ratio of (OM-ferrihydrite coprecipitates, following 90 days of reaction with 0.2 and 2.0 mM Fe(II).

Table S1: Fitting and calculated Mossbauer spectral parameters

Sample	Temp.	HWHM ¹ mm/s	δ_o ² mm/s	$\langle\Delta\rangle$ or $\langle\epsilon_o\rangle$ ³ mm/s	σ_Δ ⁴ mm/s	$\langle B_{hf}\rangle$ ⁵ Tesla	$\sigma_{B_{hf}}$ ⁶ Tesla	$\langle CS\rangle$ ⁷ mm/s	$\langle \Delta \rangle$ or $\langle\epsilon\rangle$ ⁸ mm/s	$\sigma_{(\Delta)}$ ⁹ mm/s	$\langle H \rangle$ ¹⁰ Tesla	$\sigma_{(B_{hf})}$ ¹¹ Tesla	red. χ^2 (¹²)
C/Fe = 0	RT	0.138	0.35	0.54 (32%) 0.92 (68%)	0.19 0.33	na ¹³ na	na na	0.35	0.79	0.34	na	na	0.66
	5 K	0.24	0.47	-0.004	na na	49.59 (54%) 44.4 (46%)	1.58 2.45	0.47	-0.004	na	48.1	2.58	1.63
C/Fe = 1.2	RT	0.135*	0.36	0.63 (42%) 1.01 (58%)	0.2 0.31	na na	na na	0.36	0.85	0.33	na	na	0.61
	5 K	0.25	0.47	-0.011	na na	43.2 (43%) 47.1 (57%)	3.27 2.14	0.47	-0.01	na	45.4	3.3	7.1
C/Fe = 1.6	RT	0.135*	0.36	0.64 (40%) 1.02 (60%)	0.2 0.32	na na	na na	0.36	0.86	0.33	na	na	0.6
	5 K	0.27	0.47	-0.02	na na	44.2 (77%) 26.2 (23%)	3.44 17.4	0.47	-0.017	na	40.4	10.8	1.34

¹Lorentzian half width at half maximum; ²isomer shift; ³quadrupole splitting or quadrupole shift parameter ; ⁴ Δ std dev of the component;

⁵average magnetic hyperfine field; ⁶ B_{HF} standard deviation; ⁷average center shift; ⁸absolute average quadrupole or quadrupole shift parameter;

⁹ & ¹¹ are absolute average standard deviation of Δ and B_{hf} ; ¹⁰ absolute average magnetic hyperfine field; ¹² goodness of fit; ¹³ na = not applicable

Modeling was carried out using Voigt-based fitting method of Rancourt and Ping (1991) with Recoil™ Software; * These parameters are frozen during modeling:

No coupling was allowed between CS, QS or ϵ and average B_{hf} ; the A+/A- areas of doublet are fixed at 1; A1/A3 and A2/A3 areas are fixed at 2 and 3

³A 2 Gaussian component distribution is used for quadrupole splitting, Δ (Δ of individual component and its % is shown in brackets)

³A 2 Gaussian component distribution is used for magnetic hyperfine field, B_{Hf} (B_{Hf} individual component and its % is shown in brackets)

Rancourt D.G, Ping, Y.Y. Voigt-based methods for arbitrary-shape static hyperfine parameter distributions in Mossbauer spectroscopy. *Nuclear Instruments and Methods in Physics Research* **1991**, B58, 85-97.

Table S2 Percent Fe(II) removed from solution following 18 h of reaction of 0.2 or 2 mM Fe(II) with (OM-)ferrihydrite containing C/Fe molar ratios of 0-1.6.

C/Fe molar ratio	0.2 mM Fe(II)	2 mM Fe(II)
0	59.1	18.6
0.3	56.0	17.9
0.4	53.6	17.1
0.6	50.7	15.6
0.8	48.1	14.6
1.2	47.6	13.3
1.6	44.8	12.3

Table S3 Fe concentration (mg/L) in the desorption solution following OC desorption from the initial and reacted solids.

C/Fe molar ratio	Initial Solids	Reacted Solids	
		0.2 mM Fe(II)	2 mM Fe(II)
0	0.2	0.2	0.2
0.3	0.2	0.3	0.2
0.4	0.3	0.3	0.3
0.6	0.3	0.4	0.4
0.8	0.3	1.6	3.0
1.2	0.4	1.6	3.3
1.6	0.3	3.5	6.0

Table S4 Composition of the initial DOM solution

Species	$\mu\text{mol L}^{-1}$
DOC	12500
Al	53.5
Si	88.9
Fe	22.6
Mg	33.8
Ca	40.6
Mn	3.9